npj | Materials Degradation

www.nature.com/npjmatdeg

ARTICLE OPEN

Check for updates

Weak impact of microorganisms on Ca, Mg-bearing silicate weathering

Oleg S. Pokrovsky[1,2,3]✉, Liudmila S. Shirokova[1,3], Svetlana A. Zabelina[3], Guntram Jordan[4] and Pascale Bénézeth[1]

Assessment of the microbial impact on mineral dissolution is crucial for a predictive understanding of basic (Ca, Mg bearing) silicate weathering and the associated CO_2 consumption, bioerosion, and CO_2 storage in basaltic rocks. However, there are controversies about the mechanism of microbial effect, which ranges from inhibiting via nil to accelerating. Here we studied diopside interaction with the heterotrophic bacterium *Pseudomonas reactants* and the soil fungus *Chaetomium brasiliense* using a combination of mixed-flow and batch reactors and in situ (AFM) and ex situ (SEM) microscopy. The results provide new nano-level insights into the degree to which microorganisms modify silicate dissolution. Taking into account negligible effects of organic ligands on diopside dissolution as reported earlier, we conclude that the microbial effect on Ca-Mg silicates is weak and the acceleration of dissolution of "basic" silicate rocks in the presence of soil biota is solely due to pH decrease in porewaters.

npj Materials Degradation (2021)5:51 ; https://doi.org/10.1038/s41529-021-00199-w

INTRODUCTION

Chemical weathering of basic (Ca and Mg bearing) silicates is a primary factor regulating the climate of our planet via a long-term (million year scale) CO_2 uptake from the atmosphere[1]. Both direct biological (enzymatic action of bacteria, fungi, and plant roots) and indirect physico-chemical (soil porewater pH, extracellular organic ligands and biomass degradation products) mechanisms have been identified for chemical weathering of primary silicate minerals in soil environments[2–4]. Among the "aqueous" factors, controlling the intensity of this process, solution pH, pCO_2, and organic compounds produced during enzymatic degradation of vegetation litter or the exudates of soil bacteria and plant roots are believed to be the most important[5]. The organic compounds capable to affect mineral dissolution rate include (but are not limited to) extracellular acid and neutral polysaccharides, simple carboxylic acids, uronic acids (galacturonic, guluronic), peptides, and aminoacids[6,7], as well as various lichen polyphenolic compounds[8].

Positive effects of bacteria and organic ligands on alumosilicate dissolution are fairly well established[9–15]. These effects are related to the capacity of biota to facilitate the Al-O-Si and Fe-O-Si rate-limiting bond breaking, due mostly to strong complexation of bacterially originated organic moieties with rate-controlling aqueous Al^{3+}(aq) cation[16], surface $>AlOH_2^+$ and $>FeOH_2^+$ sites[17], or Fe^{3+}(aq) mobilization in solution[18–20]. The latter is known to prevent passivation of mineral surfaces by newly formed Fe(III) hydroxides[21,22]. However, all the above mentioned mechanisms are not likely to operate for Fe- and Al-free, Ca and Mg dominant silicates. In fact, several experimental works performed over the past two decades unambiguously demonstrated the lack of any sizable impact of CO_2 and organic ligands (at otherwise constant pH) on Ca- and Mg-bearing mineral dissolution at typical soil water environments. The reason for this is rather weak complexation of organic ligands with $>CaOH_2^+$ and $>MgOH_2^+$ surface sites responsible for the rate-controlling Mg–O and Ca–O bond breaking in these minerals[23–30]. According to these studies, unreasonably high concentrations of naturally relevant organic ligands (0.01–0.1 M) are necessary to significantly enhance or inhibit mineral dissolution. As a result, the effect of extracellular organic products and in general soil biota on the weathering rate of Mg- and Ca-bearing minerals in natural settings is expected to be weak. Further, work with heterotrophic bacteria and basaltic glass[31], wollastonite[28] and olivine[32] demonstrated that even extremely high concentration of live biomass (several gram per liter, regardless of the presence of nutrients) are not capable of substantially accelerating the Ca, Mg, or Si release rate from the mineral. As a result, despite the dominant paradigm on the importance of microbes in chemical weathering of Ca-Mg-silicates in soil environments, the impact of biota on dissolution rates of these silicates might be lower than generally thought. This, in turn, may require revisiting the current understanding of biotic control on feedbacks in atmospheric CO_2 consumption vs. silicate weathering processes. To further address the role of soil biota on mineral weathering process and to extend the previous results to other alkaline-earth bearing minerals (e.g., crystalline mixed calcium and magnesium silicates), in the present study we measured the dissolution rate of typical basic silicate diopside ($CaMgSi_2O_6$) in the presence of aquatic and soil microorganisms. For these experiments, we were able to separate the effect of pH from that of bacterial presence using a mixed-flow and batch reactor systems coupled with an in situ and ex situ microscopic examination of reacted surfaces.

To provide a better understanding of the bacteria–mineral interaction in the context of chemical weathering in soils and CO_2 geological storage, we selected a common soil and underground bacterium, *Pseudomonas reactans*. Bacterial strains of the genera *Pseudomonas*, thanks to their relatively easy culturing, have been frequently used as a model organisms in studying mineral weathering in the past[33,34] and recently[15,28,35]. We also used a soil fungus, representative of saprophytic ascomycetes. Diopside was chosen as a typical model mineral for basic silicates, frequently used as a representative of silicate dissolution at the

[1]Geosciences and Environment Toulouse, UMR 5563 CNRS, University of Toulouse, 31400 Toulouse, France. [2]BIO-GEO-CLIM Laboratory, Tomsk State University, Tomsk 634050, Russia. [3]N. Laverov Federal Center for Integrated Arctic Research of the Ural Branch of the Russian Academy of Sciences, Arkhangelsk 163000, Russia. [4]Department für Geo- und Umweltwissenschaften, Ludwig-Maximilians-Universität, München, Theresienstr, 41, 80333 München, Germany. ✉email: oleg.pokrovsky@get.omp.eu

Published in partnership with CSCP and USTB

npj nature partner journals

Earth surface[36]. Indeed, because hydrolysis of Ca–O and Mg–O bonds is often the rate-limiting step for Ca- and Mg-bearing mineral dissolution[37], understanding of microorganism interaction with diopside may help to predict the reactivity of other basic silicates in the presence of microbes. In the present study, the experiments were designed in batch and flow-through reactors under constant biomass concentration, in the presence of both live and dead cells in both nutrient-free and nutrient-bearing media. We measured forward far-from equilibrium dissolution rates and we microscopically examined reacted surfaces with respect to microorganism attachment, etch pits and corrosion features. The ensemble of obtained results demonstrated rather weak impact of both bacterium and fungus on diopside reactivity, regardless of the presence of nutrients and live status of microorganisms. Moreover, the passivation of mineral surfaces via formation of an exopolysaccharide layer (in case of bacteria) may act as protection mechanism in natural settings. Globally, these new findings challenge the dominant paradigm on dominant biotic control of basic silicates weathering at the Earth surface conditions. This may require revising the quantitative modeling of chemical weathering as main factor of biotically driven long-term CO_2 consumption (coupled to Ca and Mg release from silicates). Further, the results call for a need of in situ assessment of soil porewater pH at high spatial and temporal resolution as a sole factor controlling the rate of Ca-, and Mg-bearing silicate weathering.

RESULTS

Diopside interaction with *P. reactans*

In most experiments performed at pH of 6–9, stoichiometric release of Si, Ca, and Mg was observed. In bacteria-free experiments, diopside dissolution rates decreased by ca. 0.5–1 order of magnitude during the pH decrease from 6 to 9 (Fig. 1, Table 1). The DOC concentration remained fairly stable in the course of given bacterial experiment and generally ranged from 7 to 25 mg L^{-1} being the highest at highest biomass concentration. Considering certain scatter in the rates obtained in different experiments, the presence of bacteria in either nutrient-free or nutrient-rich media did not exhibit any significant (at $p < 0.05$) effect on Si release rate from diopside, or even led to a decrease of dissolution rates (Fig. 2). In fact, the effect of bacterial presence did not exceed 0.2 log R_{Si} units, whereas the reproducibility of rates measured in individual reactors at otherwise similar aqueous solution composition ranged from 0.1 to 0.3 log R_{Si} units. Thus it can be concluded that, within the resolution of our experiments, the impact of bacteria on diopside Si dissolution rate could not be quantified or it was below 0.2 log R unit. Furthermore, there was a net inhibiting effect of bacteria on Ca and Mg release rate from the diopside in nutrient solution at pH = 6.1 (Fig. 2a). In more alkaline solutions (pH = 8.5–9.0), the presence of bacteria (with or without nutrients) did not considerably (>0.2 log R unit) impact the release rate of Si, Ca, and Mg (Fig. 2b).

The second remarkable result of BMFR experiments is that live bacteria with (D2-2, D2-3, D4-2, D4-3) and without (D1-2, D1-3, D3-2, D3-3) nutrients exhibited a negligible effect of biomass concentration (between 0.54 and 3.85 g_{wet}/L) on Mg, Ca and Si release rates because there was no substantial (>0.2 log R unit) change in rate during biomass increase by a factor of 7 (Table 1).

The third important observation is that there was a significant, by a factor of 3–5, decrease in Ca, Mg, Si concentrations and release rates between the beginning (exp. D1-1, D2-1, D3-1, and D4-1) and the end of bacteria-free experiments (exp. D1-4, D2-4, D3-4, and D4-4). This is illustrated in Supplementary Fig. 1, where the Si concentration in the outlet solution corresponding to the sequence of inlet solutions "bacteria-free 0.1 M NaCl → 0.54 g_{wet}/L bacteria → 3.85 g_{wet}/L bacteria → bacteria-free 0.1 M NaCl", at a constant flow rate, demonstrated a 3- to 5-fold decrease between the initial and the final bacteria-free experiment. Such a decrease could be related to passivation of mineral surface by bacterial cells and their exometabolites as evidenced from in situ microscopic observations (see section on the AFM observations below).

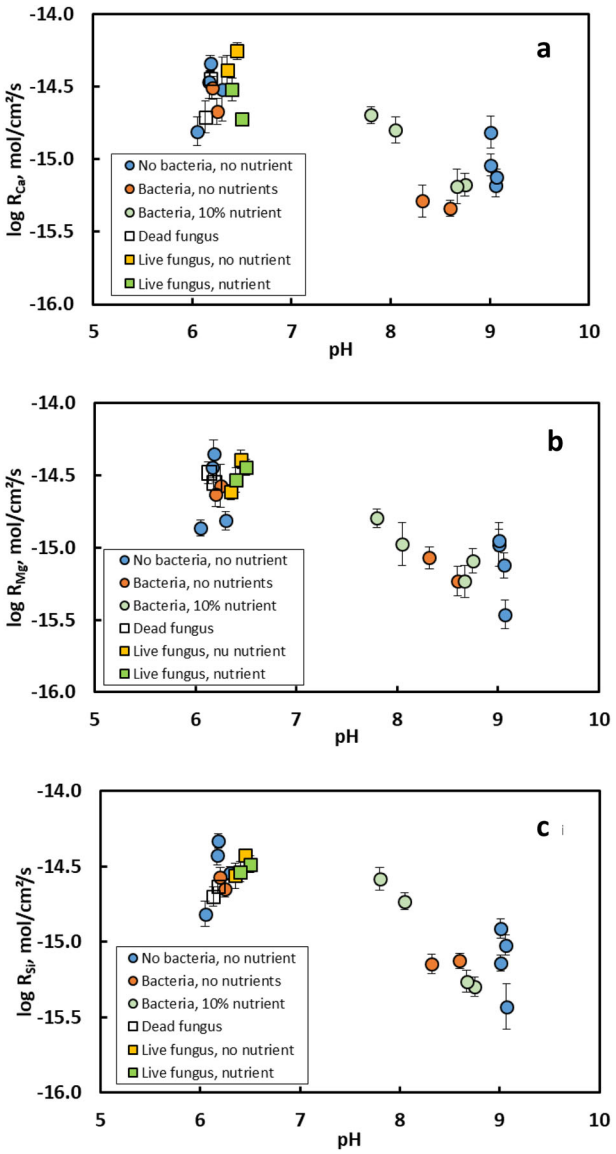

Fig. 1 Results of diopside dissolution in experimental reactors. Calcium (**a**), Mg (**b**), and Si (**c**) release rates from diopside measured in the mixed-flow reactor with and without bacteria and 10% nutrient or nutrient-free solution and in the batch reactor in the presence of fungus.

Ca, Mg, and Si release in the presence of fungus

Results of Ca, Mg, and Si release from diopside in 0.1 M NaCl and in nutrient media in the presence of live and dead *Chaetomium brasiliense* demonstrated that concentrations of all mineral constituents increase quasi-linearly with time in all types of experiments (illustrated for Si in Supplementary Fig. 2). The linear regression coefficients varied from 0.9 to 0.99 for Si and from 0.8 to 0.95 for Ca and Mg. The pH remained generally constant (±0.2 unit) or slightly increased (within 0.2–0.3 units) over the 19 days of exposure. In batch experiments with fungus, the DOC increased

Table 1. Results of Bacterial MFR experiment. *R* units are mol cm^{-2} s^{-1}.

	Experiment	pH	log R_{Ca}	log R_{Mg}	log R_{Si}
D1-1	0.1 M NaCl + 0.01 M MES, no bacteria, no nutrients	6.18	−14.34 ± 0.055	−14.35 ± 0.10	−14.33 ± 0.050
D2-1	0.1 M NaCl + 0.01 M MES, no bacteria, no nutrients	6.17	−14.47 ± 0.110	−14.44 ± 0.075	−14.42 ± 0.061
D2-4	0.1 M NaCl + 0.01 M MES, no bacteria, no nutrients	6.05	−14.81 ± 0.10	−14.86 ± 0.055	−14.81 ± 0.085
D1-4	0.1 M NaCl + 0.01 M MES, no bacteria, no nutrients	6.30	−14.52 ± 0.22	−14.81 ± 0.065	−14.54 ± 0.045
D3-4	0.1 M NaCl + 0.01 M NaHCO3, no bacteria, no nutrients	9.01	−15.04 ± 0.075	−14.98 ± 0.15	−15.14 ± 0.056
D3-1	0.1 M NaCl + 0.01 M NaHCO3, no bacteria, no nutrients	9.06	−15.18 ± 0.078	−15.12 ± 0.085	−15.02 ± 0.065
D4-1	0.1 M NaCl + 0.01 M NaHCO3, no bacteria, no nutrients	9.07	−15.12 ± 0.055	−15.46 ± 0.10	−15.43 ± 0.15
D4-4	0.1 M NaCl + 0.01 M NaHCO3, no bacteria, no nutrients	9.01	−14.82 ± 0.11	−14.95 ± 0.075	−14.91 ± 0.065
D1-2	0.1 M NaCl + 0.01 M MES, 0.54 g/l bacteria, no nutrients	6.25	−14.67 ± 0.089	−14.57 ± 0.15	−14.65 ± 0.052
D1-3	0.1 M NaCl + 0.01 M MES, 3.85 g/l bacteria, no nutrients	6.20	−14.51 ± 0.078	−14.63 ± 0.082	−14.57 ± 0.065
D3-2	0.1 M NaCl + 0.01 M NaHCO3, 0.54 g/l bacteria, no nutrients	8.60	−15.34 ± 0.055	−15.23 ± 0.10	−15.13 ± 0.05
D3-3	0.1 M NaCl + 0.01 M NaHCO3, 3.85 g/l bacteria, no nutrients	8.32	−15.29 ± 0.11	−15.07 ± 0.075	−15.15 ± 0.065
D2-2	0.1 M NaCl + 0.01 M MES, 0.54 g/l bacteria, 10% NB	7.80	−14.70 ± 0.058	−14.80 ± 0.065	−14.58 ± 0.075
D2-3	0.1 M NaCl + 0.01 M MES, 3.85 g/l bacteria, 10% NB	8.05	−14.80 ± 0.089	−14.97 ± 0.15	−14.73 ± 0.055
D4-2	0.1 M NaCl + 0.01 M NaHCO3, 0.54 g/l bacteria, 10% NB	8.75	−15.18 ± 0.078	−15.09 ± 0.085	−15.30 ± 0.065
D4-3	0.1 M NaCl + 0.01 M NaHCO3, 3.85 g/l bacteria, 10% NB	8.67	−15.19 ± 0.12	−15.23 ± 0.11	−15.26 ± 0.072

R units are mol cm^{-2} s^{-1}.

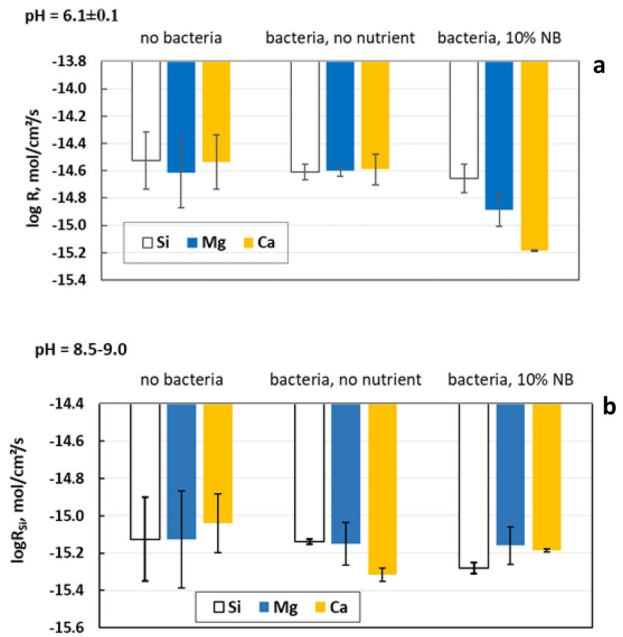

Fig. 2 Results of diopside dissolution in the presence of heterotrophic bacteria. Synthesis of obtained steady-state Ca, Mg, and Si release rates (average ± s.d.) from diopside at pH 6 (**a**) and 8.5–9.0 (**b**) with and without *Pseudomonas reactans* and in the presence or not of nutrients. The error bars represent average of 2–4 duplicates, each comprising 3–4 independent sampling at the steady state.

from 10 to 30 mg/L over the first 100 h of reaction and then remained constant over the following 300 h. Taking into account that (1) all solutions are strongly undersaturated with respect to diopside, all other possible Ca and Mg silicates and amorphous silica, and (2) there is no effect of aqueous Ca, Mg, and Si concentration on diopside forward dissolution rates in neutral solution[24,38,39], one can quantify the far-from equilibrium dissolution rate (*R*) for each individual experiment using the following equation, which can be applied over the whole duration of the experiment:

$$R = \left(d[\mathrm{Ca, Mg, Si}/2]_{\mathrm{tot}}/dt\right)/s \quad (1)$$

where *t* (s) designates the elapsed time, $[Ca, Mg, Si]_{tot}$ (mol/L) stands for the concentration of calcium, magnesium or silica released from the solid, and s (cm^2/L) is the powder B.E.T. surface area. Results are listed in Table 2. The uncertainties on these rates stem from duplicate experiments and range between ±10 and 30%. The rates measured in the presence of dead or live fungi generally agree (within ±0.2 log units) with those of abiotic and biotic experiments in mixed-flow reactor (Fig. 1). The Si release rates were a factor of 1.5 higher in experiments with live fungus (with or without nutrients) compared to experiments with dead fungus (Fig. 3). However, there was no difference in Mg release rate between different treatments, whereas the Ca release rate, although more variable among replicates, exhibited a maximum in nutrient-free experiments with live fungus (Fig. 3). The element release rate in the presence of fungus was mostly stoichiometric (Table 2). The disagreement between Si and Mg release rate ranged from 0.1 to 0.05 log *R* unit except in one experiment with dead biomass (0.2 units). Calcium release rate was in agreement with that of Si within 0.01–0.19 log *R* units, except in one experiment with live biomass (0.24 log *R* lower).

AFM observations in the presence of *P. reactans*

Freshly reacted diopside surfaces (2–5 h in sterile NaCl solution) largely preserved their cleavage plane morphology (Fig. 4A). Occasionally, some etch pits and local surface roughness were observable (Fig. 4B). After 36 h reaction in bacteria-free nutrient solution, rounding of edges occurred (Fig. 4C). After 1–2 days of reaction with nutrient solution at pH = 8.5 or 6.5, we have observed a strong colonization of diopside surfaces by a biofilm-like bacterial assemblage (Fig. 4D). This extracellular polymeric substances (EPS) coverage included individual elongated spheres and generally convex forms, less than 0.5 µm in longest axis, although their size distribution was not uniform (Fig. 4D–F). Groups of objects occasionally exhibited a distinct internally preferred orientation, which was, however, quite variable within a

Table 2. Results of fungus batch experiments (0.1 M NaCl).

Experiment	pH	log R_{Mg}	log R_{Ca}	log R_{Si}
Dead biomass, 4.46 g/L	6.18	−14.55 ± 0.10	−14.44 ± 0.054	−14.63 ± 0.051
Dead biomass, 4.95 g/L	6.13	−14.48 ± 0.074	−14.71 ± 0.11	−14.70 ± 0.065
Live biomass, 4.83 g/L, no nutrient	6.35	−14.62 ± 0.055	−14.39 ± 0.10	−14.56 ± 0.085
Live biomass, 5.1 g/L, no nutrient	6.45	−14.39 ± 0.065	−14.25 ± 0.058	−14.43 ± 0.045
Live biomass, 5.6 g/L live, 1% nutrient	6.50	−14.44 ± 0.055	−14.73 ± 0.045	−14.49 ± 0.054
Live biomass, 5.1 g/L, live, 1% nutrient	6.40	−14.53 ± 0.085	−14.52 ± 0.078	−14.54 ± 0.067

R units are mol cm^{-2} s^{-1}.

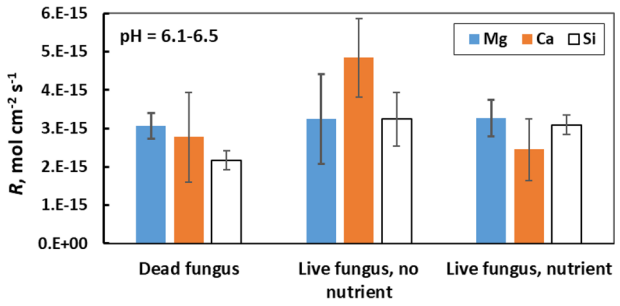

Fig. 3 Synthesis of obtained Ca, Mg, and Si release rates (average ± s.d., mol cm^{-2} s^{-1}) from diopside at pH 6.0–6.5 with and without *Chaetomium brasiliense* fungus (4.5–5.6g_{wet}/L) and in the presence or not of nutrients (1% Czapek medium). The error bars represent average of two reactors, each comprising 9–10 independent sampling as a function of time over 19 days of exposure.

relatively small area (~50 μm^2). The obtained images are consistent with earlier reported bacterial EPS via AFM[40,41]. Extensive production of exopolymeric substances precluded imaging of individual bacterial cells within this thick biofilm coverage. In contrast, mineral interaction with bacteria in nutrient-free neutral electrolyte allowed recognizing individual cells attached to the diopside surface (Fig. 4G); however, no site of preferential interactions such as steps or edges could be identified.

SEM imaging of diopside reacted with fungus

The diopside grains reacted with dead fungus in 0.1 M NaCl demonstrated sharp borders and no clear dissolution features (Fig. 5a). After reaction with live fungus in nutrient-free media, there was an appearance of specific dissolution features such as etching and rounding of edges (Fig. 5b). The rounded edges were also observed in experiments with live fungus; these features were distinctly different from cleavage (Fig. 5c). The diopside crystals were also imaged in the presence of fungal mycelium: the hyphae were strongly attached to the grain surfaces and not lost during sample preparation for SEM (Fig. 5d). Some grains appeared significantly (>50%) covered by or even embedded into network of fungal hyphae. There were no distinct sites of hyphae location at the diopside surface, and overall, the interaction appeared to be quite inert, nonspecific and site-indifferent. With increasing the resolution, some organic spherical entities, 2–3 µm in diameter, were identified at the extremities of the hyphae (Fig. 5d).

DISCUSSION

Results of the present study demonstrated a weak (or nonmeasurable) impact of bacterium and fungus on Ca, Mg, and Si release rate from diopside. Biologically accelerated weathering of silicates is thought to be controlled by microbial production of extracellular enzymes, chelates, simple, and complex organic acids and exopolysaccharides[5,11,42–44]. However, there are serious controversies, whether such an effect is largely direct (metabolically driven nutrient mobilization and specific ligand production) or indirect (passive pH lowering and cation complexation via EPS excretion), given that it is largely dependent on the nature of mineral and the identity of microorganism[9,45–48]. Furthermore, considering basic silicates, some studies reported nil or inhibiting effect of bacteria on olivine[32,49,50] or wollastonite[28] dissolution, whereas other claimed strong accelerating effect of fungi on olivine[21,22,51]. However, in the latter works, all the effects of microorganisms were limited to their ability to sequester rate-inhibiting Fe(III) thus preventing the slowdown of dissolution, rather than directly promoting the breaking of structural bonds in the mineral lattice. Overall, in contrast to large number of works on microbial impact on alumosilicate dissolution[52–56], the interaction of aquatic microorganisms and relevant organic ligands with Ca or Mg-bearing silicates remained insufficiently characterized.

In the present study, the global rate uncertainty in the studied pH range (6–9) was between 20 and 50%. This uncertainty stems from both the pH variation (±0.2–0.3 units) during the course of an experiment and the reproducibility of steady-state concentrations of diopside constituents in mixed-flow reactors with bacteria-free systems or among duplicates in batch reactors with dead fungus (±20%). Therefore, we conclude that the difference between abiotic (bacteria-free or dead cells) and live bacteria experiments is within the experimental uncertainty. As such, the effect of selected live microorganisms on Ca, Mg, and Si release rate from diopside is not significant, or cannot be resolved using the experimental design employed in the present study.

In this regard, the present result corroborates the former works of our group, which demonstrated weak inhibiting or negligible impact of cultivable heterotrophic bacteria *P. aureofaciens* on wollastonite[28] and *P. reactans* on basaltic glass[31] and olivine[32], in agreement with other studies[15,47,49]. The broad meaning of these results is that microbial impact on basic silicate mineral dissolution is limited by (i) pH decrease, thus accelerating proton-promoted dissolution, which is relevant to all basic silicates; (ii) release of Fe (III)-complexing organic ligands including siderophores. The latter is pertinent solely to minerals whose dissolution is limited by Fe $(OH)_3$ passivation of the surface. In all other cases of microbially affected basic silicate dissolution, the concentrations of excreted organic ligands are not sufficient to sizably complex Mg and Ca at the surface or in the aqueous solution, which is necessary for breaking of rate-controlling Mg–O or Ca–O bonds at the mineral surface. For example, gluconic acid and its derivatives are believed to be the main exometabolite of heterotrophic bacteria that use glucose as a substrate[10,34]. Gluconic acid can favor olivine dissolution in neutral waters[32]; however, this effect occurs at concentrations >1 mM, totally irrelevant to natural environments. Another example comes from a concerted study of ~40 various ligand impact on wollastonite dissolution[28]. These authors

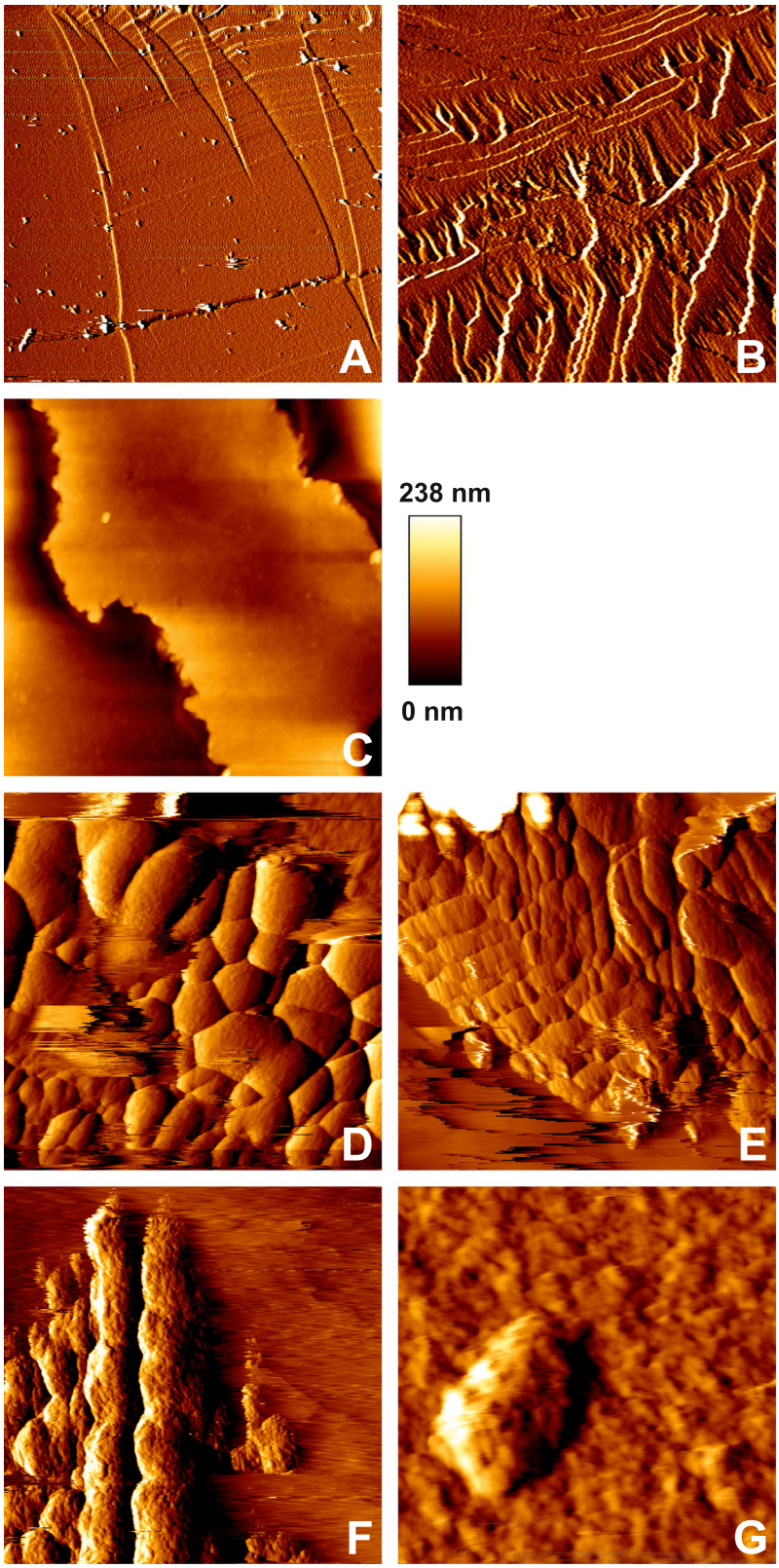

Fig. 4 Atomic Force Microscopy (AFM) images of diopside. A–C In situ AFM images of diopside surfaces immersed within sterile electrolyte media for up to 5 h (**A** 70 × 70 μm², deflection mode; **B** 20 × 20 μm², deflection mode; **C** 12 × 12 μm², height mode—with the color scale spanning a total of 238 nm). **D–G** In situ AFM images of diopside surfaces immersed in nutrient media (**D** 8.6 × 8.6 μm², deflection mode; **E** 10 × 10 μm², deflection mode; **F** 5.5 ×5.5 μm², deflection mode; **G** 1.5 × 1.5 μm², deflection mode.

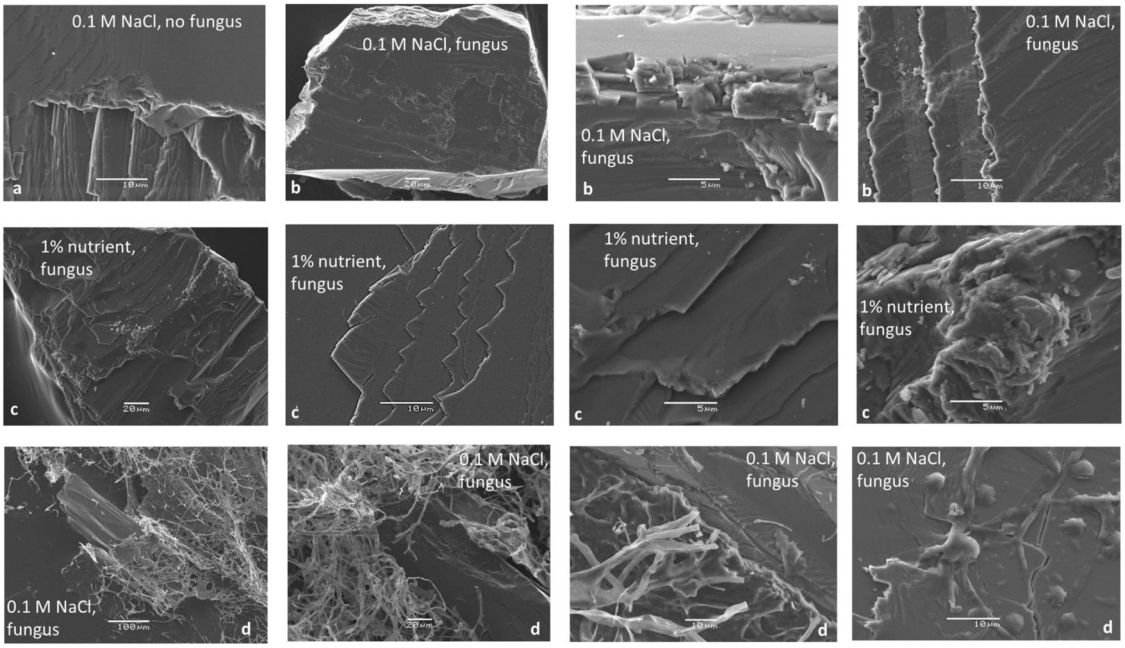

Fig. 5 Scanning Electron Microscope (SEM) images of diopside. SEM images of reacted diopside surfaces in the sterile electrolyte (**a**), live fungus in 0.1 M Na Cl (**b, d**), and in 1% nutrient media (**c, d**).

calculated, based on the results in mixed-flow reactors, the threshold concentration of ligands necessary to triple the rates of wollastonite at pH around 7. For most ligands, very high concentration (2–3 orders of magnitude higher than those encountered in natural settings) were necessary to appreciably affect the rates. Finally, Golubev and Pokrovsky (2006)[24] demonstrated that very high concentrations (0.01–0.1 M) of organic ligands originated from enzymatic degradation of organic matter or bacterial metabolic activity, are necessary to appreciably affect diopside dissolution. Considering these results and by analogy with olivine and wollastonite, we hypothesize that possible impacts of studied heterotrophic bacteria on the diopside dissolution via gluconic acid or other soluble exometabolite products are not detectable due to insufficient concentration of these compounds generated via metabolism of *P. reactans* in experimental reactors.

Below we discuss the mechanisms of diopside interaction with microbial cells and natural implications. Reactive surfaces in both bacterial and fungal experiments demonstrated lack of specific sites of dissolution, etch pit formation, surface amorphization or new mineral occurrences. Rather, our in situ (AFM) and ex situ (SEM) microscopic observations suggested "passivation" of reacted surfaces by microbial metabolic products. We therefore hypothesize that the biofilm coverage either limited aqueous solution contact with mineral surface or merely did not produce sufficient amount of organic ligands capable to impact the diopside dissolution.

Microbial biofilm formation, dominated by exopolysaccharides (EPS), is known to protect the mineral surface from interaction with bulk fluid[42,46,47,57] thus inhibiting overall dissolution rate[2,3,6,7,35,58]. In the present experiments with diopside, the biofilm formation was also evidenced from indirect assessment of dissolution rate: the rates decreased by a factor of 2–3 after ~500 h treatment with bacteria; this decrease persisted even after changing back the inlet solution to sterile bacteria-free background electrolyte (see Supplementary Fig. 1). Noteworthy that such an irreversible rate decrease was also observed after reaction with live bacteria in nutrient-free media and suggested substantial and long-lasting interaction of live *P. reactans* with diopside surface in both neutral (pH = 6) and slightly alkaline (pH = 9) solutions. At the same time, no decrease in diopside dissolution rate was observed over 400–800 h of experiments in the abiotic inorganic systems[23,24].

As a result of lack of measurable rate increase in the presence of either bacteria or fungus in this range of pH, nutrient and biomass concentration, we suggest, in agreement with previous studies, that, regardless of nutrient regime, biomass concentration and vital status of microorganism, solely the solution pH can act as the main governing factor of mineral dissolution in the presence of aquatic microorganisms. A similar conclusion has been recently achieved for olivine dissolution in the presence of complex natural microbial communities[59]. Therefore, implementation of mineral–microorganism interaction in chemical weathering codes requires solely the information on porewater solution chemistry that can be directly assessed from macroscopic measurements of interstitial soil solutions.

Moreover, extremely high concentrations of organic ligands, necessary to affect the rates of basic silicate dissolution in laboratory experiments[24,28,32], together with high bacterial and fungi concentrations, comparable with those used in the present study, can be encountered exclusively in surface (litter) soil horizons, and unlikely to ever occur in deep (mineral) soil horizons. Exceptions are specific microenvironments around fungal hyphae, or near decaying organic matter. For example, a strong acidification was reported with hyphae bound to the biotite surface[60]. To quantify these effects on a broader scale, high-resolution in situ quantitative analysis of chemical composition of solution, bacteria, and organic ligand concentration in soil pore water microenvironments are needed.

At the same time, the role of microorganisms under natural environment, especially in the nonsaturated zone, might be more important than that in aqueous environment of mixed-flow experiments. It is generally understood that a lack of "wetted" mineral surface area, or mineral surfaces being exposed to the reactive fluid, could be a partial explanation for slower reaction rates observed in the field compared to those measured in the laboratory with unlimited water[61,62]. For example, via exerting hydrated exopolysaccharides, microbial cells are capable of prolonging the degree of mineral surfaces hydration during natural wetting/drying cycles. Therefore, although our

experiments, performed under nutrient-free conditions with starved cells, are most similar to natural environments under short-term scale, there is sizable uncertainty in extrapolating these short-term laboratory results to long-term field conditions. The latter are known to exhibit one to three orders of magnitude lower weathering rates, due to different timescale of observation, diversity of microorganisms, and nutritional conditions.

For more general natural implications of the obtained results, we consider below all Ca, Mg-bearing 'basic' silicates including Ca alumosilicates. Several lines of evidences allow us to suggest rather weak effect of dissolved organics on (Ca, Mg, Al)-bearing silicate dissolution in natural settings. First, the concentration range of various carboxylic ligands (oxalic, citric, malonic, succinic, lactic, formic, acetic), detected in soil solutions, spans from 10^{-6} to 10^{-4} M[63]. Laboratory experiments suggest that these concentrations are still not sufficient to appreciably affect feldspars dissolution rates. Second, the effect of organic ligands on Al release and thus on overall dissolution rates of feldspars and basaltic glass is absent or becomes negligible at pH ≥ 7[16,64]. The pH of rivers and streams draining 'basic' silicate rocks is between 7 and 8[65,66] whereas the pH of soil solutions in organic-rich soils typically ranges from 4 to 7[67]. However, surficial acid- and organic-rich soil horizons rarely contain primary silicates, whereas in deep (C) soil horizons, the interstitial soil solution pH is always above 7 (see ref. [65]). At these conditions, the effect of organic ligands on Ca, Mg, Al, and Si release rate from primary silicates should be negligible, which corroborates the conclusion of Drever (1994)[68] that vegetation should cause an increase in weathering rate through the pH effect only where the pH is below 4–5. As a results, the sole effect of soil organics on both acidic and felsic rock weathering seems to be in decreasing the aqueous activity of Al^{3+} thus preventing formation of secondary minerals without significant modification of Ca and Mg ions release.

It has been widely argued that the presence of soluble minerals in trace amounts in the rocks (i.e., carbonates[69]; phosphates[70] may strongly affect the intensity of chemical weathering and export fluxes of major ions. The effect of biological activity in this case is expected to be solely due to pH decrease in the vicinity of microorganisms or plant roots. Indeed, the data for dolomite[25], calcite and magnesite[27,29], brucite[26], and calcite[30] dissolution in the presence of various organics demonstrate a negligible effect of organic ligands on Ca and Mg release from carbonates and oxides at environmentally relevant conditions.

The effect of soil and atmospheric pCO_2 is always considered to be an important factor accelerating rock weathering at the Earth surface. In this regard, we would like to underline that this effect stems solely from the decrease of soil solution pH since there is no chemical effect of CO_2(aq) or dissolved H_2CO_3 molecules on the main rock-forming silicates dissolution rate[39], and in neutral and alkaline solutions the pCO_2 effect becomes even inhibiting[71].

Overall, this work allows a better understanding of microbially affected basic silicate dissolution and provides microscopic insights for quantifying the degree to which the heterotrophic bacteria and fungi are capable of modifying the dissolution rate of rock-forming silicates. Using bacterial mixed-flow and batch reactors combined with in situ atomic force microscopy of bacteria-diopside surfaces and experiments on diopside dissolution in the presence of fungus combined with microscopic examination of reacted surfaces, we demonstrated a rather weak impact of microorganisms on Ca, Mg, and Si release rate. Regardless of the presence or absence of nutrients, in a wide range of pH (from 6 to 9) and despite very high biomass concentration (up to 4–5 g_{wet}/L), the rates were not considerably affected by microbial presence. Moreover, there was a detectable (ca. by a factor of 3) decrease in reactivity of diopside after its prolonged contact with live heterotrophic bacteria. This 'passivation' of the mineral surface was evidenced by extensive production of exopolymeric substances yielding a biofilm-like coverage already after 1–2 days of interaction in nutrient-rich media. Despite tight contact between fungus and diopside surfaces, no site of preferential interactions such as steps, kinks or edges, etch pits or surface amorphization was detected. The obtained results are fully consistent with large body of evidences that any possible microbially produced organic ligands at concentrations relevant to live biotic systems or natural settings are not capable of noticeably impacting the reactivity of Mg–O and Ca–O sites on diopside surface. As such, this work challenges the dominant paradigm of an overwhelming role of biota on silicate mineral weathering in soils. At the same time, it is in line with a controversial opinion of Sverdrup (2009)[72] that physical and chemical conditions of forest soils do not allow any significant direct surface actions on minerals by microorganisms or tree roots. While we do not contest the importance of microbial organic matter in Fe and Al complexation and mobilization from silicate structure, the role of biota on basic (Ca and Mg) silicates, playing a pivotal role in atmospheric CO_2 sequestration via chemical weathering, may be much lower than traditionally thought. In fact, only drastic pH decrease (i.e., over several pH units), probably occurring in the microniches adjacent to plant roots, is capable of sizably (>a factor of 2–3) increase mineral dissolution rate. It is not excluded, however, that this promoting effect will be partially attenuated due to biofilm formation and passivation of silicate surfaces by microbial cells. Detecting such 'active' or 'passive' microniches within the complex plant-microbe-mineral systems and more importantly, characterizing chemical environment of the fluids with spatial resolution on the level of μm to mm may turn out to be a bottleneck for quantitative mechanistic modeling of chemical weathering. Currently, these gradients are not taken into account even in most sophisticated modeling approaches[73,74]. Further experimental and field studies are thus needed to answer the question whether a quantitative modelling of basic silicate mineral weathering and related CO_2 consumption require an explicit prediction for microbial activity or it can be merely approximated by the pH of bulk soil porewaters.

METHODS

Mineral, bacterial, and fungal culture

Natural diopside ($Ca_{0.99}Mg_{0.98}Fe_{0.02}Cr_{0.01}Si_2O_6$) crystals characterized in previous works[24,39] were used in this study. Ultrasonically cleaned 100–200 μm size fraction having a specific surface area of 1045 ± 50 cm^2/g was selected for dissolution rate measurements.

Pseudomonas reactans is a common rod-shape groundwater and soil bacteria averaging 2 μm in size (see further description in refs. [31,32]). For experiments, cells were first cultured to a stationary stage on a shaker at 25 °C in the darkness using 10% nutrient broth with the following composition: 0.1 g/L glucose, 1.5 g/L peptone, 0.6 g/L NaCl, and 0.3 g/L yeast extract. Cells were allowed starving for 2 days in nutrient-free media, prior the macroscopic dissolution and microscopic (AFM) experiments. For this, freshly grown cell suspension (at the stationary stage) was rinsed by sterile 0.6 g L^{-1} NaCl solution via centrifugation, and then placed in 0.6 g L^{-1} NaCl without nutrients for 2 days. Before the experiment, this bacterial suspension was rinsed again with sterile 0.6 g L^{-1} NaCl to remove, as possible, all cellular exometabolites.

Active bacteria number counts (colony forming-units, CFU/mL) were performed using Petri dish inoculation on a nutrient agar (0.1, 0.2, and 0.5 mL of sampled solution in three replicates) in a laminar hood box. Inoculation of blanks was routinely performed to assure the absence of external contamination. The biomass of live bacteria suspensions was also quantified by measuring wet (after it was centrifuged 15 min at 10,000 rpm) and freeze-dried weights in duplicates. Before the experiments, cells were rinsed twice in either the appropriate fresh culture media or a sterile 0.1 M NaCl solution using centrifugation with ~500 mL of solution for 1 g of wet biomass, to remove adsorbed metals and cell exudates from the surface. The conversion ratio wet/freeze-dried weight of *P. reactans* was equal to 8.4 ± 0.5. The conversion factor of optical density (600 nm, 10 mm path) and wet biomass (g_{wet}/L) to the cell number (CFU/mL) was equal to (5 ± 1)×10^8 and (8.0 ± 1.5)×10^7, respectively, as

determined by triplicate measurements. Typical live biomass concentration during experiments was 0.54 and 3.85 g_{wet}/L.

Experiments on fungus were performed with *Chaetomium brasilience*, belonging to the largest genus of saprophytic ascomycetes, inhabiting soils worldwide. The environmental habitats of genus *Chaetomium* include deserts, salterns, agricultural, mangrove, living plants and animals, air, decayed wood, and stones[75]. *Chaetomium brasilience* Bat. Et Pontual 1948, stumm F-3649 was obtained from All-Russian Collection of Microorganisms —VKM (http://www.vkm.ru/Collections.htm). Fungal biomass was produced on liquid Czapek medium (3 g/L $NaNO_3$, 1 g/L K_2HPO_4, 0.5 g/L KCl; 0.5 g/L $MgSO_4 \times 7H_2O$, 0.01 g/L $FeSO_4 \times 7H_2O$, 30 g/L saccharose at pH = 6.0). The biomass was centrifuged at 5000 rpm during 15 min, rinsed four times in 0.1 M NaCl and allowed starving during 2 days in 0.1 M NaCl prior the experiment. Dead (heat-killed) cells were produced via autoclaving 1 h at 132 °C the freshly grown fungal biomass followed by thorough rinsing in sterile 0.1 M NaCl. Cell concentration in the sample was analyzed by measuring optical density (OD) at 580 nm using a spectrophotometer, with the culture medium used as a reference. Diopside dissolution experiments were performed in duplicates, in 0.1 M NaCl with dead biomass, and live biomass with and without 1% nutrient solution.

Bacterial mixed-flow reactor

The Bacterial Mixed-Flow Reactor (BMFR) system used in this work was similar to the one used for basaltic glass dissolution in the presence of bacteria[31]. The Teflon-made 25 mL reactor with a suspended Teflon-coated stirbar, immersed in a water bath at 25 ± 0.5 °C, was fitted with 20 µm poresize Magna Millipore Nylon outlet filters (45 mm diameter) to allow bacteria to pass while retaining the 100–200 µm mineral powder in the reactor. This system therefore maintained a constant biomass concentration in the reactor, equal to that of the inlet fluid. The input fluids were kept in 1 L polypropylene bottles closed with Biosilico® ventilated caps. These fluids were stirred continuously during the experiments and were changed typically each 7 days. This allowed maintenance of a constant and stable stationary phase bacterial culture in the bacteria-bearing inlet fluid. Bacteria concentration was verified by periodical sampling of inlet and outlet fluids for cell optical density (total biomass) and live cell numbers (via agar plate counting). Prior to each experiment, all reactor system parts, including tubing, were sterilized at 130 °C for 30 min and rinsed with sterile MilliQ water.

Steady-state dissolution rates (R_i, mol/cm²/s) were computed from measured solution composition using:

$$R_i = -q \cdot 1/n \cdot \Delta[i(\mathrm{aq})]_{\mathrm{tot}}/s \quad (2)$$

where q (L/s) designates the fluid flow rate, $\Delta[i(\mathrm{aq})]_{\mathrm{tot}}$ (mol/L) stands for the difference between the input and output solution concentration of ith element, n is the stoichiometric coefficient of ith element in diopside formula equaled to 2, 1, and 1 for Si, Mg and Ca, respectively, and s (cm²) refers to the total mineral surface area present in the reactor. The surface area used to calculate the rates was that measured on the fresh (unreacted) diopside powder. Note that during 600 h of reaction time, no systematic variation of the surface area for powder reacted at 5 < pH < 10 in bacteria-free solutions was observed[24].

Experiments were performed in series at constant flow rate between 0.018 and 0.022 mL/min. This corresponded to a mechanical steady-state achievement (×5 reactor volume renewal) after 4–5 days. At the beginning of each series, a quantity of fresh diopside powder was added to the reactor system. For each experimental series, a sterile bacteria-free 0.1 M NaCl with relevant buffer (10 mM NaMES (2-morpholinoethanesulfonic acid) or $NaHCO_3$) was first prepared and injected into the reactor until a steady-state outlet fluid composition was attained (typically 2 weeks, D1 series). Once steady state was attained, live bacteria (0.54 g_{wet}/L) with or without nutrients were added to this inlet solution (D2 series). The next series comprised higher concentration of live bacteria in the inlet fluid (3.85 g_{wet}/L). The 2nd and 3rd series lasted 7–10 days each. After that, the inlet solution was replaced by fresh sterile bacteria-free fluid; this experiment, which lasted >3 weeks, was destined to assess the recovery of the mineral reactivity and to test the consequences of passivation of mineral surface by a bacterial biofilm.

The inlet solutions were composed of 0.1 M NaCl and 0.01 M NaMES (D1 and D2 series) and 0.1 M NaCl with 0.01 M $NaHCO_3$ (D3 and D4 series). The 1:10 diluted Aldrich nutrient broth (0.1 g/L glucose, 1.5 g/L peptone, 0.6 g/L NaCl, and 0.3 g/L yeast extract) was added to selected live bacteria experiments. These were compared to live bacteria experiments performed without nutrients. Overall, the experiments conducted in this study can be divided into three main categories: (1) bacteria- and nutrient-free, (2) live bacteria in nutrient-free media, and (3) live bacteria in 10% growth media.

All outlet sample fluids were additionally filtered through 0.45 µm Millipore acetate cellulose filters and acidified with ultrapure 2% HNO_3 before chemical analysis. The inlet fluids were routinely analyzed at the beginning, in the middle and at the end of each experiment and were filtered and processed using exactly the same protocol as the outlet fluids.

Mechanical steady-state was achieved after 24 h of reaction. For each steady-state condition, minimum four independent measurements of Mg, Ca, and Si concentrations, bacterial optical density, pH, and flow rate were performed (reproducibility of ±10%) and used for calculating the dissolution rate. The cell count (CFU) on nutrient agar plates was performed at the beginning, in the middle and at the end of each experimental run and did not vary significantly throughout all experiments.

Batch experiments on diopside dissolution in the presence of fungus

The aim of these experiments was to compare, under identical solution conditions, the Ca, Mg, and Si release rate from diopside placed in contact with dead and live fungus cultures. The batch reactors used to study diopside–fungus interaction consisted of sterile 250 mL polypropylene culture flasks with vented caps (Biosilico). All manipulations were conducted in a sterile laminar hood box (class 100). For experiments, 1.3 g of sterilized 100–200 µm diopside were placed in 250 mL sterile solution. We conducted six experiments in duplicates, four involving live cultures, with and without 1% nutrient solution, and two with dead (autoclaved) biomass (in nutrient-free 0.1 M NaCl).

The reactors were inoculated with 4.2–5.6 g_{wet}/L of fresh *Chaetomium brasiliense* culture or the equivalent amount of dead biomass and placed on rotative shaker (120 rpm) at 25 ± 1 °C for 19 days. Sterile controls were routinely run both for nutrient media and 0.1 M NaCl solutions and did not demonstrate any fungal contamination. Periodically, 10 mL aliquots of homogeneous mineral suspension + fungus were collected using sterile serological pipettes and transferred in polystyrene vials for Ca, Mg, Si, pH, and cell biomass measurements. The mineral/fluid ratio remained constant during experiments and the concentration of fungus was not affected by the sampling. Calcium, Mg and Si concentrations were analyzed in 0.45 µm filtrates and pH and cell biomass were measured in unfiltered samples.

Analyses

All input and output solutions were analyzed for Mg, Ca, Si, optical density, and pH as a function of time. NIST buffers (pH = 4.008, 6.865, and 9.180 at 25 °C) were used for calibration of a combination pH-electrode (Schott Geräte H62). Magnesium and Ca concentrations were measured by flame atomic absorption spectroscopy with an uncertainty of 1 and 2% and a detection limit of 0.1 and 0.2 µM, respectively. Total silica concentration was determined by a Technicon automatic analyzer using the molybdate blue method with an uncertainty of 2% and a detection limit of 0.3 µM. The concentration of soluble organic exometabolites of bacteria and fungi was measured as total dissolved organic carbon (DOC) using a TOC Shimadzu VSCN analyzer with an uncertainty of 5% and a detection limit of 0.1 mg C_{org} L^{-1}. All experiments were performed at far-from equilibrium conditions with respect to diopside as calculated via vMinteq program[76] with relevant solubility parameters[77].

Microscopic observations

An AFM study using a biological instrument (JPK NanoWizard) allowed in situ high-resolution characterization of the status of diopside surfaces in the presence of live bacteria with and without nutrients. Diopside cleavage planes were obtained by cleaving optically transparent crystals 5–10 mm in size in a laminar hood box (A100). Fresh cleavage surfaces were sterilized by alcohol and fixed within petri dishes for imaging with the AFM. For long-term (>5 h) exposure, diopside cleavages were reacted under sterile conditions with 1 g_{wet}/L of bacterial biomass in separate petri dishes. The petri dishes were mounted into the AFM for in situ inspection of the diopside surfaces directly immersed within the bacteria containing medium, removed from the microscope for further storage, and reinvestigated with the microscope whenever appropriate. Depending on the specific aim of the scanning process (attempt of potentially imaging all adhering matter on the surface vs. attempt of removing matter adhering to the surface), images were acquired with both

intermittent-contact mode and contact mode using uncoated Si-cantilevers with integrated tips.

The diopside grains reacted with fungus were examined by Scanning Electron Microscopy (SEM). Prior to characterization by SEM, samples were centrifuged (3000 × *g*, 30 min) and the organic matter was removed from the solid phase by rinsing them in nutrient-free sterile 0.1 M NaCl solution. The remaining solids were rinsed three times with MilliQ water and freeze-dried at −60 °C. They were observed after carbon film coated on the sample surface with a JEOL JSM 6360LV SEM coupled with a SDD PGT Sahara EDS analyzer operating at 30 kV.

DATA AVAILABILITY

Supplementary material is available. All measured dissolution rates are presented in Tables 1 and 2. Other relevant data are also available from the corresponding author of this paper upon a reasonable request.

Received: 16 June 2021; Accepted: 11 September 2021;
Published online: 28 September 2021

REFERENCES

1. Berner, R. A. Weathering, plants and the long-term carbon cycle. *Geochim. Cosmochim. Acta* **56**, 3225–3231 (1992).
2. Hutchens, E., Valsami-Jones, E., McEldowney, S., Gaze, W. & McLean, J. The role of heterotrophic bacteria in feldspar dissolution—an experimental approach. *Min. Mag.* **67**, 1157–1170 (2003).
3. Hutchens, E. Microbial selectivity on mineral surfaces: possible implications for weathering processes. *Fungal Biol. Rev.* **23**, 115–121 (2009).
4. Li, Z. B. et al. Specificity of low molecular weight organic acids on the release of elements from lizardite during fungal weathering. *Geochim. Cosmochim. Acta* **256**, 20–34 (2019).
5. Barker, W. W., Welch, S. A. & Banfield, J. F. Biogeochemical weathering of silicate minerals. *Rev. Mineral. Geochem.* **35**, 391–428 (1997).
6. Ullman, W. J., Kirchman, D. L., Welch, S. A. & Vandevivere, P. H. Laboratory evidence for microbially mediated silicate mineral dissolution in nature. *Chem. Geol.* **132**, 11–17 (1996).
7. Welch, S. A., Barker, W. W. & Banfield, J. F. Microbial extracellular polysaccharides and plagioclase dissolution. *Geochim. Cosmochim. Acta* **63**, 1405–1419 (1999).
8. Adamo, P. & Violante, P. Weathering of rocks and neogenesis of minerals associated with lichen activity. *Appl. Clay Sci.* **16**, 229–256 (2000).
9. Barker, W. W., Welch, S. A., Chu, S. & Banfield, J. F. Experimental observations of the effects of bacteria on aluminosilicate weathering. *Am. Mineral.* **83**, 1551–1563 (1998).
10. Welch, S. A. & Ullman, W. J. The effect of microbial glucose metabolism on bytownite feldspar dissolution rates between 5° and 35 °C. *Geochim. Cosmochim. Acta* **63**, 3247–3259 (1999).
11. Bennett, P. C., Rogers, J. R. & Choi, W. J. Silicates, silicate weathering, and microbial ecology. *Geomicrobiol. J.* **18**, 3–19 (2001).
12. Van Hees, P. A. W., Lundström, U. S. & Mörth, C.-M. Dissolution of microcline and labradorite in a forest O horizon extract: the effect of naturally occurring organic acids. *Chem. Geol.* **189**, 199–211 (2002).
13. Neaman, A., Chorover, J. & Brantley, S. L. Effects of organic ligands on granite dissolution in batch experiments at pH 6. *Am. J. Sci.* **306**, 451–473 (2006).
14. Ganor, J., Reznik, I. J. & Rosenberg, Y. O. Organics in water-rock interactions. *Rev. Mineral. Geochem.* **70**, 259–369 (2009).
15. Ahmed, E. & Holmström, S. J. M. Microbe-mineral interactions: the impact of surface attachement on mineral weathering and element selectivity by microorganisms. *Chem. Geol.* **403**, 13–23 (2015).
16. Oelkers, E. H. & Schott, J. Does organic acid adsorption affect alkali-feldspar dissolution rates? *Chem. Geol.* **151**, 235–245 (1998).
17. Stumm, W. Reactivity at the mineral-water interface: dissolution and inhibition. *Colloids Surf. A* **120**, 143–166 (1997).
18. Schalscha, E. B., Appelt, M. & Schatz, A. Chelation as a weathering mechanism: 1. Effects of complexing agents on the solubilisation of Fe from minerals and granodiorite. *Geochim. Cosmochim. Acta* **31**, 587–596 (1967).
19. Liermann, L. J., Kalinowski, B. E., Brantley, S. L. & Ferry, J. G. Role of bacterial siderophores in dissolution of hornblende. *Geochim. Cosmochim. Acta* **64**, 587–602 (2000).
20. Bonneville, S. et al. Plant-driven fungal weathering: early stages of mineral alteration at the nanometer scale. *Geology* **37**, 615–618 (2009).
21. Gerrits, R. et al. How the rock-inhabiting fungus *K. petricola* A95 enhances olivine dissolution through attachment. *Geochim. Cosmochim. Acta* **282**, 76–97 (2020).
22. Gerrits, R. et al. High-resolution imaging of fungal biofilm-induced olivine weathering. *Chem. Geol.* **559**, 119902 (2021).
23. Golubev, S. V., Bauer, A. & Pokrovsky, O. S. Effect of pH and organic ligands on the kinetics of smectite dissolution at 25 °C. *Geochim. Cosmochim. Acta* **70**, 4436–4451 (2006).
24. Golubev, S. V. & Pokrovsky, O. S. Experimental study of the effect of organic ligands on diopside dissolution kinetics. *Chem. Geol.* **235**, 377–389 (2006).
25. Pokrovsky, O. S. & Schott, J. Kinetics and mechanism of dolomite dissolution in neutral to alkaline solutions revisited. *Am. J. Sci.* **301**, 597–626 (2001).
26. Pokrovsky, O. S., Schott, J. & Castillo, A. Kinetics of brucite dissolution at 25 °C in the presence of organic and inorganic ligands and divalent metals. *Geochim. Cosmochim. Acta* **69**, 905–918 (2005).
27. Pokrovsky, O. S., Golubev, S. V. & Jordan, G. Effect of organic and inorganic ligands on calcite and magnesite dissolution rates at 60 °C and 30 atm pCO_2. *Chem. Geol.* **265**, 33–43 (2009).
28. Pokrovsky, O. S., Shirokova, L. S., Bénézeth, P., Schott, J. & Golubev, S. V. Effect of organic ligands and heterotrophic bacteria on wollastonite dissolution kinetics. *Am. J. Sci.* **309**, 731–772 (2009).
29. Jordan, G., Pokrovsky, O. S., Guichet, X. & Schmahl, W. W. Organic and inorganic ligand effects on magnesite dissolution at 100 °C and pH = 5 to 10. *Chem. Geol.* **242**, 484–496 (2007).
30. Oelkers, E. H., Golubev, S. V., Pokrovsky, O. S. & Benezeth, P. Do organic ligands effect calcite dissolution rates? *Geochim. Cosmochim. Acta* **75**, 1799–1813 (2011).
31. Stockmann, G. J. et al. Does the presence of heterotrophic bacteria *Pseudomonas reactans* affect basaltic glass dissolution rates? *Chem. Geol.* **296-297**, 1–18 (2012).
32. Shirokova, L. S. et al. Experimental study of the effect of heterotrophic bacterium (*Pseudomonas reactans*) on olivine dissolution kinetics in the context of CO_2 storage in basalts. *Geochim. Cosmochim. Acta* **80**, 30–50 (2012).
33. Webley, D. M., Duff, R. B. & Mitchell, W. A. Plate method for studying the breakdown of synthetic and natural silicates by soil bacteria. *Nature* **188**, 766–767 (1960).
34. Duff, R. B., Webley, D. M. & Scott, R. O. Solubilization of minerals and related materials by 2-ketogluconic acid-producing bacteria. *Soil Sci.* **95**, 105–114 (1962).
35. Aouad, G., Crovisier, J.-L., Geoffroy, V. A., Meyer, J.-M. & Stille, P. Microbially-mediated glass dissolution and sorption of metals by *Pseudomonas aeruginosa* cells and biofilm. *J. Haz. Mat.* **B136**, 889–895 (2006).
36. Brantley, S. L. & Chen, Y. Chemical weathering rates of pyroxenes and amphiboles. *Rev. Mineral.* **31**, 119–172 (1995).
37. Schott, J., Pokrovsky, O. S. & Oelkers, E. H. The link between mineral dissolution/precipitation kinetics and solution chemistry. *Rev. Mineral. Geochem.* **70**, 207–258 (2009).
38. Knauss, K. G., Nguyen, S. N. & Weed, H. C. Diopside dissolution kinetics as a function of pH, CO_2, temperature, and time. *Geochim. Cosmochim. Acta* **57**, 285–294 (1993).
39. Golubev, S. V., Pokrovsky, O. S. & Schott, J. Experimental determination of the effect of dissolved CO_2 on the dissolution kinetics of Mg and Ca silicates at 25 °C. *Chem. Geol.* **217**, 227–238 (2005).
40. Van der Aa, B. C. & Dufrene, Y. F. In situ characterization of bacteria extracellular polymeric substances by AFM. *Coll. Surf. B Biointerfaces* **23**, 173–182 (2002).
41. Beech, I. B., Smith, J. R., Steele, A. A., Penegar, I. & Campbell, S. A. The use of atomic force microscopy for studying interactions of bacterial biofilms with surfaces. *Coll. Surf. B Biointerfaces* **23**, 231–247 (2002).
42. Chen, J., Blume, H. P. & Beyer, L. Weathering of rocks induced by lichen colonization—a review. *Catena* **39**, 121–146 (2000).
43. Buss, H. L., Luttge, A. & Brantley, S. L. Etch pit formation on iron silicate surfaces during siderophore-promoted dissolution. *Chem. Geol.* **240**, 326–342 (2007).
44. Uroz, S., Calvaro, C., Turpault, M.-P. & Frey-Klett, P. Mineral weathering by bacteria: ecology, actors and mechanisms. *Trends Microbiol.* **17**, 378–387 (2009).
45. Vandevivere, P., Welch, S. A., Ullman, W. J. & Kirchman, D. L. Enhanced dissolution of silicate minerals by bacteria at near-neutral pH. *Microb. Ecol.* **27**, 241–251 (1994).
46. Welch, S. A. & Vandevivere, P. Effect of microbial and other naturally occurring polymers on mineral dissolution. *Geomicrobiol. J.* **12**, 227–238 (1994).
47. Roberts, J. A. Inhibition and enhancement of microbial surface colonization: the role of silicate composition. *Chem. Geol.* **212**, 313–327 (2004).
48. Tourney, J. & Ngwenya, B. T. The role of bacterial extracellular polymeric substances in geomicrobiology. *Chem. Geol.* **386**, 115–132 (2014).
49. Oelkers, E. H. et al. The efficient long-term inhibition of forsterite dissolution by common soil bacteria and fungi at Earth surface conditions. *Geochim. Cosmochim. Acta* **168**, 222–235 (2015).
50. Garcia, B. et al. An experimental model approach of biologically-assisted silicate dissolution with olivine and Escherichia coli—impact on chemical weathering of mafic rocks and atmospheric CO_2 drawdown. *Appl. Geochem.* **31**, 216–227 (2013).

51. Pokharel, R., Gerrits, R., Schuessler, J. A. & von Blankenburg, F. Mechanisms of olivine dissolution by rock-inhabiting fungi explored using magnesium stable isotopes. *Chem. Geol.* **525**, 18–27 (2019).
52. Wu, L., Jacobson, A. D., Chen, H.-C. & Hausner, M. Characterization of elemental release during microbe-basalt interactions at T = 28 °C. *Geochim. Cosmochim. Acta* **71**, 2224–2239 (2007).
53. Wu, L. L., Jacobson, A. D. & Hausner, M. Characterization of elemental release during microbe-granite interactions at T=28 degrees C. *Geochim. Cosmochim. Acta* **72**, 1076–1095 (2008).
54. Hausrath, E. M., Neman, A. & Bratnley, S. L. Elemental release rates from dissolving basalt and granite with and without organic ligands. *Am. J. Sci.* **309**, 633–660 (2009).
55. Daval, D. Carbon dioxide sequestration through silicate degradation and carbon mineralisation: promises and uncertainties. *npj Mater. Degrad.* **2**, 11 (2018).
56. Voelz, J. L., Johnson, N. W. & Chun, C. L. Quantitative dissolution of environmentally accessible iron residing in iron-rich minerals: a review. *ACS Earth Space Chem.* **3**, 1371–1392 (2019).
57. Lee, J.-U. & Fein, J. B. Experimental study of the effects of *Bacillus subtilis* on gibbsite dissolution rates under near-neutral pH and nutrient-poor conditions. *Chem. Geol.* **166**, 193–202 (2000).
58. Lüttge, A. & Conrad, P. G. Direct observation of microbial inhibition of calcite dissolution. *Appl. Environ. Microbiol.* **70**, 1627–1632 (2004).
59. Wild, B., Imfeld, G., Guyot, F. & Daval, D. Early stages of bacterial community adaptation to silicate aging. *Geology* **46**, 555–558 (2018).
60. Bonneville, S. et al. Tree-mycorrhiza symbiosis accelerate mineral weathering: evidences from nanometer-scale elemental fluxes at the hypna-mineral interface. *Geochim. Cosmochim. Acta* **75**, 6988–7005 (2011).
61. Yokoyama, T. & Nishiyama, N. Role of water film in weathering of porous rhyolite under water unsaturated condition. *Proc. Earth Planet. Sci.* **7**, 916–919 (2013).
62. Harrison, A. L., Dipple, G. M., Power, I. M. & Mayer, K. U. Influence of surface passivation and water content on mineral reactions in unsaturated porous media: Implications for brucite carbonation and CO_2 sequestration. *Geochim. Cosmochim. Acta* **148**, 477–495 (2015).
63. Hongve, D., Van Hees, P. A. W. & Lundstrom, U. S. Dissolved components in precipitation water percolated through forest litter. *Eur. J. Soil Sci.* **51**, 667–677 (2000).
64. Oelkers, E. H. & Gislason, S. R. The mechanism, rates and consequences of basaltic glass dissolution: I. An experimental study of the dissolution rates of basaltic glass as a function of aqueous Al, Si and oxalic acid concentration at 25 °C and pH = 3 and 11. *Geochim. Cosmochim. Acta* **65**, 3671–3681 (2001).
65. Pokrovsky, O. S., Schott, J., Kudryavtzev, D. I. & Dupré, B. Basalt weathering in Central Siberia under permafrost conditions. *Geochim. Cosmochim. Acta* **69**, 5659–5680 (2005).
66. Dessert, C., Gaillardet, J., Dupré, B., Schott, J. & Pokrovsky, O. S. Fluxes of high- versus low-temperature water-rock interactions in aerial volcanic areas: the example of the Kamchatka Peninsula, Russia. *Geochim. Cosmochim. Acta* **73**, 148–169 (2009).
67. Berner, E. K. & Berner, R. A. *Global environment: Water, Air, and Geochemical Cycles* (Prentice Hall, 1996).
68. Drever, J. I. The effect of land plants on weathering rates of silicate minerals. *Geochim. Cosmochim. Acta* **58**, 2325–2332 (1994).
69. White, A. F., Bullen, T. D., Davison, V. V., Schulz, M. S. & Clow, D. W. The role of disseminated calcite in the chemical weathering of granitoid rocks. *Geochim. Cosmochim. Acta* **63**, 1939–1953 (1999).
70. Goddéris, Y. et al. Modelling weathering processes at the catchment scale: the WITCH numerical model. *Geochim. Cosmochim. Acta* **70**, 1128–1147 (2006).
71. Schott, J. et al. Formation, growth and transformation of leached layers during silicate minerals dissolution: the example of wollastonite. *Geochim. Cosmochim. Acta* **98**, 259–281 (2012).
72. Sverdrup, H. Chemical weathering of soil minerals and the role of biological processes. *Fungal Biol. Rev.* **23**, 94–100 (2009).
73. Godderis, Y., Schott, J. & Brantley, S. L. Reactive transport models of weathering. *Elements* **15**, 103–106 (2019).
74. Maher, K. & Mayer, K. U. Tracking diverse minerals, hungry organisms, and dangerous contaminants using reactive transport models. *Elements* **15**, 81–86 (2019).
75. Abdel-Azeem, A. in *Fungal Biology, Recent Developments on Genus Chaetomium* (ed. A. M. Abdel-Azeem) 3–77. (Springer Nature Switzerland AG, 2020).
76. Gustafsson, J. *Visual MINTEQ Ver. 3.1.* http://vminteq.lwr.kth.se (2014).
77. Dixit, S. & Carroll, S. A. Effect of solution saturation state and temperature on diopside dissolution. *Geochim. Trans.* **8**, 3 (2007).

ACKNOWLEDGEMENTS

Supports from grants BIOCASTRO of MITI (CNRS) and CaBioCa of Défi (Action conjointe, MITI CNRS) are acknowledged.

AUTHOR CONTRIBUTIONS

O.S.P. developed the concept of the study. L.S.S., S.A.Z. and O.S.P. performed dissolution experiments. G.J. performed AFM study. P.B. participated in laboratory experiments and SEM study. O.S.P. wrote the paper, with input from L.S.S., P.B., G.J. and S.A.Z. All the co-authors discussed the final version of the paper.

COMPETING INTERESTS

The authors declare no competing interests.

ADDITIONAL INFORMATION

Supplementary information The online version contains supplementary material available at https://doi.org/10.1038/s41529-021-00199-w.

Correspondence and requests for materials should be addressed to Oleg S. Pokrovsky.

Reprints and permission information is available at http://www.nature.com/reprints

Publisher's note Springer Nature remains neutral with regard to jurisdictional claims in published maps and institutional affiliations.